Effects of External pH on Binding of External Sulfate, 4,4′-dinitro-stilbene-2,2′-disulfonate (DNDS), and Chloride to the Band 3 Anion Exchange Protein

SI-QIONG JUNE LIU, ELIZABETH RIES, and PHILIP A. KNAUF

From the Department of Biophysics, University of Rochester School of Medicine and Dentistry, Rochester, New York 14642

ABSTRACT A model in which two positively-charged titratable sites enhance the affinity for anionic substrates can explain the increase in external iodide dissociation constant (K_o^I) with increasing pH_o (Liu, S. J., F.-Y. Law, and P. A. Knauf. 1996. *J. Gen. Physiol.* 107:271–291). If sulfate binds to the same external site as I^-, this model predicts that the $SO_4^=$ dissociation constant (K_o^S) should also increase. The data at pH_o 8.5 to 10 fit this prediction, and the pK for the titration is not significantly different from that (pK_C) for the low-pK group that affects K_o^I. The dissociation constant for the apparently competitive inhibitor, DNDS (4,4′-dinitro-stilbene-2,2′-disulfonate), also increases greatly as pH_o increases. Particularly at high pH_o, a noncompetitive inhibition by DNDS is also evident. Increasing pH_o from 7.2 to 11.2 increases the competitive dissociation constant by 700-fold, but the noncompetitive is only increased ~20-fold. The pK values for these effects are similar to pK_C for K_o^I, as expected if DNDS binds near the external transport site, but it seems likely that additional titratable groups also affect DNDS binding. The apparent affinity for external Cl^- is also affected by pH_o, in a manner similar to that observed for I^-. Pretreatment with the amino-selective reagent, bis-sulfosuccinimidyl suberate (BSSS), decreases the apparent Cl^- affinity at pH 8.5, but two titrations are still evident, the first (lower) of which decreases the apparent Cl^- affinity, and the second of which surprisingly increases it. Thus, the BSSS-reactive amino groups (probably Lys-539 and Lys-851) do not seem to be involved in the titrations that affect Cl^- affinity. In general, the data support the concept that a positively charged amino group (or groups), together with a guanidino group, plays an important role in the binding of substrates and inhibitors at or near the external transport site.

INTRODUCTION

In the preceding paper (Liu et al., 1996), we have shown that the I^- dissociation constant (K_o^I) for the E_o form of band 3 (the conformation with the transport site facing outward) increases dramatically with increasing external pH (pH_o). The data can be most simply interpreted in terms of a model in which a positively charged amino acid residue with a pK of 9.5 ± 0.2 (probably lysine) contributes to binding of external substrates (Liu et al., 1996). The data are also compatible with a model similar to that proposed by Bjerrum (1992), with two titratable sites, one with a pK value of 9.3 ± 0.3 and another with a pK > 11. The lower pK residue is probably a lysine, while the higher pK site is likely arginine. Bjerrum also proposed an alternate model in which both sites are arginines.

In addition to monovalent anions such as Cl^- and I^-, the red cell anion exchange system also transports divalent anions such as $SO_4^=$ (Schnell et al., 1977; Ku et al., 1979; Milanick and Gunn, 1982). Competition experiments demonstrate that $SO_4^=$ ions bind at or near the same external transport site as do Cl^- and I^-. Also, external disulfonic stilbenes such as DNDS (4,4′-dinitro-stilbene-2,2′-disulfonate) and H_2DIDS (4,4′-diisothiocyano-dihydro-stilbene-2,2′-disulfonate) appear to act primarily as competitive inhibitors of Cl^- exchange (Fröhlich, 1982; Shami et al., 1978), suggesting that they also bind to the external-facing transport site.

If titratable positive charges contribute to the free energy of binding of monovalent anions to the external transport site, then these charges should also have an effect on the binding of divalent anions or competitive inhibitors to the same site. The affinities of these latter

Address correspondence to Dr. Philip A. Knauf, Department of Biophysics, University of Rochester Medical Center, 601 Elmwood Avenue, Rochester, NY 14642.

 J. GEN. PHYSIOL. © The Rockefeller University Press • 0022-1295/96/02/293/14 $2.00
Volume 107 February 1996 293–306

agents should be affected by external pH in a manner which is predictable from the pK values determined from the I^- affinity data.

In this paper, we test these predictions by examining the pH_o dependence of $SO_4^=$, Cl^-, and DNDS affinity. To test the hypothesis that certain amino groups are involved in external substrate binding, we also examine the effects of an amino-selective reagent, bis-sulfosuccinimidyl suberate (BSSS), on the apparent external Cl^- affinity. The results of these tests in general support the titratable substrate binding site model (Bjerrum, 1992; Liu et al., 1996), but do not rule out the possiblity that other titratable sites may play a role in the binding of at least some of these anions.

METHODS

Cell Preparation and Flux Measurement

Red blood cells were obtained from freshly drawn human blood and washed three times with 150 KH (150 mM KCl, 24 mM sucrose and 20 mM HEPES (*N*-2-hydroxyethylpiperazine-*N'*-2-ethanesulfonic acid), pH 7.2 at 0°C). The Cl^- exchange fluxes (J) were determined by measuring ^{36}Cl efflux, as described in the accompanying paper (Liu et al., 1996).

Sulfate and DNDS (4,4'-dinitrostilbene-2,2'-disulfonate) Inhibition

$SO_4^=$ is a substrate for band 3 but is transported at a much lower rate than Cl^- (~20,000 times slower at 8°C and pH 6.3 [Ku et al., 1979]). It acts as a competitive inhibitor of Cl^- exchange (Milanick and Gunn, 1982). Therefore the apparent external $SO_4^=$ dissociation constant, K_o^S, for the conformation (E_o) of band 3 with unloaded transport site facing outward was determined by the method of Milanick and Gunn (1982) from the x value of the intersection point of two Dixon plots for $SO_4^=$ inhibition with different $[Cl_o]$, as described in detail for I^- in the preceding paper (Liu et al., 1996). This same method was also used to determine K_e for the nontransported inhibitor DNDS (ICN Pharmaceuticals, Plainview, NY).

The flux media were a combination of 0 KH (339 mM sucrose and 5 mM buffer), 165 KH (165 mM KCl, 9 mM sucrose, and 5 mM buffer), and 110 mM $K_2SO_4^=$ or 0.1 mM DNDS. HEPES was used as the buffer for pH_o 7.2 to 8.5; CHES (2[*N*-cyclohexylamino]ethane sulfonic acid, from Research Organics, Inc., Cleveland, OH) for pH_o 9 to 10.5, and CAPS (3-[cyclohexylamino]-1-propane sulfonic acid, from Sigma Chemical Co., St. Louis, MO) for pH_o values higher than 10.5. The flux media were titrated with 1 M bicarbonate-free KOH.

Measurement of Transport Parameters for External Chloride

The unidirectional Cl^- efflux of control cells with ~150 mM $[Cl_i]$ was measured in media with different $[Cl_o]$, with sucrose replacing Cl^-, as described in the preceding paper. The data were fitted to the Michaelis-Menten equation by nonlinear least squares to calculate J^{mo}, the flux with maximal (saturating) $[Cl_o]$, and $K_{1/2o}$, the $[Cl_o]$ that gives half-maximal flux.

BSSS (Bis-sulfosuccinimidyl suberate) Treatment

BSSS (Pierce Chemical Co., Rockford, IL) was freshly dissolved in 150 KH at pH 7.4 at room temperature. Cells were washed once with 150 KH (pH 7.4 at room temperature), and then incubated with 2.7 mM BSSS in 150 KH at ~50% hematocrit at pH 7.25 and 37°C for 1 h. The reaction was stopped by adding 40 ml of 50 mM glycine in 150 KH (pH 7.2 at 0°C) to the reaction medium. Then the BSSS treated cells were washed three times with 150 KH (pH 7.2 at 0°C) containing 0.2% BSA (BSA, Sigma Chemical Co.). After each wash, the resuspended cells were left at room temperature for 10 min to allow the pH_i to reach equilibrium.

Data Analysis

Enzfitter (Elsevier Biosoft), a nonlinear regression data analysis program for the IBM PC, was used to fit the data for Cl^- flux, J, as a function of inhibitor concentration, [Inh], to the equation for hyperbolic inhibition, $J = J_u/(1 + [Inh]/ID_{50})$, where J_u is the uninhibited flux and ID_{50} is the [Inh] which causes 50% inhibition of the flux. Simple weighting (same error assumed for all points) was used. K_e was then calculated as the negative of the x value of the intersection point of Dixon plot lines ($1/J$ vs [Inh]) with different $[Cl_o]$, using the equations of the lines resulting from the ID_{50} and J_u values obtained by nonlinear fitting.

The dissociation constants for $SO_4^=$, DNDS, and Cl^- at various pH_o values were fitted to a model in which the affinity change is related to titration of one or two sites, as described by Eqs. 1 and 2 of the preceding paper (Liu et al., 1996). Because the variations in the dissociation constants in general increase with the size of the constants, the data were weighted according to the inverse of their values, and nonlinear least squares estimates of the parameters were obtained by using Origin (MicroCal Software, Northampton, MA).

RESULTS AND DISCUSSION

Effects of pH_o on Anions Other Than Iodide

The titratable substrate binding site (SBS) model postulates that the electrostatic field of positive charges near the external transport site contributes significantly to the binding affinity for anionic substrates, such as I^- (Liu et al., 1996). According to this model, titration of the positive charges should also affect the binding of other substrates or competitive inhibitors to the external transport site. Because of the different charges or locations of these other ions, however, the effects of pH_o may show quantitative differences, although the pK values for the titrations should not be significantly different.

The dissociation constant for binding, K_d, is related to the free energy of binding by the equation:

$$\Delta G = RT \ln K_d . \quad (1)$$

In general, ΔG is a complicated function of the interactions between the ion and the binding site. In the present context, however, we are primarily concerned with the effect of addition or removal of a positive

charge near the binding site. For a single positive charge, the electrical contribution to the free energy (in kilocalories per mole) of an anion located at a distance r from the center of the titratable positive charge is equal to the electrostatic work and is given by (Gabler, 1978):

$$\Delta G_{el} = -331.9\ n/Dr, \quad (2)$$

where n is the charge of the anion (e.g., one for a univalent anion) and D is the dielectric constant. If we write Eq. 1 for the condition when the residue is protonated (subscript +) and when it is deprotonated (subscript 0), the dissociation constant for the protonated form, K_+, and for the deprotonated form, K_0, have the following relationship, provided that the entire free energy difference between the two forms is given by ΔG_{el}:

$$\Delta G_{el} = RT\ln(K_+/K_0). \quad (3)$$

If a different anion, designated by *, is bound near the titratable charge, we can write equations for this ion similar to Eqs. 2 and 3. When these equations are solved simultaneously, we obtain:

$$K_+/K_0 = (K^*_+/K^*_0)^{(nr^*/n^*r)}. \quad (4)$$

That is, the ratio of dissociation constants in the two states for one anion is proportional to the same ratio for the other anion (*), raised to a power that is directly proportional to the ratio of the charges of the anions (n/n^*) and inversely proportional to the ratio of the distance between each anion and the positive charge (r/r^*).

Effects of pH_o on Sulfate Affinity

According to Eq. 4, if a divalent anion such as $SO_4^=$ is bound to the external transport site, and if the distance between the center of the $SO_4^=$ and the titratable positive charge is less than twice the distance between the charge and bound I^-, the doubling of n (for $SO_4^=$) relative to n^* (for I^-) in Eq. 4 predicts that the ratio of neutral and alkaline form dissociation constants for $SO_4^=$ should be larger than that for I^-. Thus, qualitatively pH_o would be expected to have a larger effect on the dissociation constant for $SO_4^=$, K_o^S, than on that for I^-, K_o^I. Because of the complex nature of the equation describing the titration (see Liu et al., 1996), however, the apparent values of K_o^I and K_o^S at each pH_o will not follow Eq. 4. As mentioned in the preceding paper (Liu et al., 1996), larger values of K_0 relative to K_+ will cause the inflection point for the pH_o titration to shift to higher pH_o values. At $pH_o < 10.5$, therefore, the predicted results for divalent and monovalent ions are quite similar (e.g., compare *solid triangles* for I^- in Fig. 3 with *dashed line* predicted for a divalent ion at the same position as I^-). Despite this apparent pK shift, numerical fits to the one-site or two-site SBS model should give pK values for $SO_4^=$ similar to those seen for I^-.

To test the SBS model, therefore, we measured K_o^S at various pH_o values. Like K_o^I, K_o^S was determined from the negative of the x value of the intersection point of Dixon plots (1/flux vs $[SO_{4o}]$) at different $[Cl_o]$ (Milanick and Gunn, 1986; Fröhlich and Gunn, 1986; Knauf and Brahm, 1989). Fig. 1 shows that the Dixon plots for $SO_4^=$ inhibition were nearly perfectly linear, indicating a single site of inhibition, as required for the determination of K_o^S.

Table I shows K_o^S as a function of pH_o. K_o^S increases markedly as pH_o is raised from 8.5 to 10, which is qualitatively consistent with the pH_o dependence of K_o^I. This increase in K_o^S is not related to the titratable site with a pK of 5.03, described by Milanick and Gunn (1982), which causes a ninefold increase in $SO_4^=$ affinity when it is protonated. Because of this site, the apparent K_o^S increases with an apparent pK of 5.99. By pH 8.5, however, the lowest pH_o shown in Table I, this titration should be over 99% complete. Thus, the titratable site characterized by Milanick and Gunn (1982) has no effect on K_o^S in the pH_o range examined here.

As shown in Table I, when K_o^I and K_o^S at various pH_o are divided by their values at pH_o 8.5, the ratio for $SO_4^=$ shows a dependence on pH_o that is similar to but somewhat stronger than that seen for I^-. This is fairly consistent with the SBS model, suggesting that the reduction

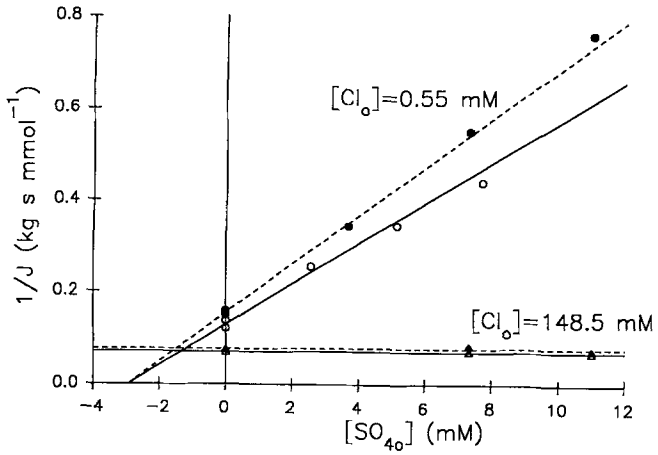

FIGURE 1. Dixon plot of inhibition of Cl^- exchange by external $SO_4^=$ at pH 8.5, 0°C. Cells were loaded with ^{36}Cl and efflux was measured into media with various $SO_4^=$ concentrations, as described in Methods. Circles represent data with $[Cl_o] = 0.55$ mM and triangles data with $[Cl_o] = 148.5$ mM. Open symbols and solid lines are for one experiment; closed symbols and dashed lines for a different experiment. Lines were drawn using the parameters for single-site hyperbolic inhibition obtained from nonlinear least-squares fits (using Enzfitter) to the original flux vs $SO_4^=$ data. The dissociation constant for external $SO_4^=$ binding to the external-facing transport site, K_o^S, is given by the negative of the x value of the intersection point for the lines with low and high $[Cl_o]$, and is nearly the same for the two experiments.

of local positive charge by titration may explain the decrease in both $SO_4^=$ and I^- binding affinity with pH_o. The effect of pH_o on K_o^S, however, is somewhat larger than predicted for a divalent ion at the same location as I^- (in which case the ratios for $SO_4^=$ and I^- should be nearly identical at $pH_o \leq 10$), suggesting that $SO_4^=$ may interact with an additional titratable charge. The idea that $SO_4^=$ and I^- are not located in precisely the same place when bound to the external transport site is supported by evidence that $SO_4^=$ and Cl^- interact differently with an inhibitor, NAP-taurine (*N*-[4-azido-2-nitrophenyl]-2-aminoethylsulfonate) (Fröhlich and Gunn, 1987; Knauf et al., 1978).

If the favorable electrostatic free energy resulting from interaction of this positive charge with anions were the dominant factor in determining the total binding free energy, and if I^- and $SO_4^=$ were bound at exactly the same position, one would expect divalent anions such as $SO_4^=$ to have a higher apparent affinity for the external transport site than do monovalent anions such as I^- (Eqs. 1 and 2). The fact that the dissociation constants are higher for $SO_4^=$ than for I^- (Table I), indicating a lower affinity for the doubly charged ion, demonstrates that factors other than the electrostatic interaction make important contributions to the binding free energy.

pK for Dependence of K_o^S on pH_o

If the seven determinations of K_o^S between pH_o 8.5 and 10 (Table I) are fitted to a single-site titration curve, the pK value is 8.7 (± 1.0). A fit to a two-site model, with the pK for the higher pK residue (D) set to 11.35 (Bjerrum, 1992), also gives a pK for the lower pK (C) residue of 8.7 ± 1.0. Because of the limited data range, these pK's are not very accurately determined, but they are not far from the pK values (9.5 ± 0.2 or 9.3 ± 0.3) determined by fitting similar models to the data for the pH_o dependence of K_o^I (Liu et al., 1996). The pK value is very close to that (8.7) determined by Bjerrum (1992) from measurements of Cl^- fluxes under conditions of low ionic strength. The simplest interpretation of the similar pK values would be that $SO_4^=$, I^-, and Cl^- interact with the same titratable positive charge.

Although the data fit well with the SBS model, this is not the only model which could explain the increase of $SO_4^=$ dissociation constants with pH_o. A model in which positive fixed charges act to increase the local concentration of anions near the transport site, without themselves participating in substrate binding, predicts qualitatively similar results. In this case, the ratio of local anion concentration to that in the bulk medium is governed by the electrical potential between the local region and the bulk medium. The equilibrium distribution ratio of divalent anions ($SO_4^=$) between the local and bulk regions, given by the Nernst equation, will thus be the square of the corresponding distribution for monovalent anions (I^-) at each value of pH_o. Table I shows that this relationship does not hold for pH_o 10 as compared to pH_o 8.5, providing evidence against this simple version of the fixed charge model. As discussed

TABLE I

Comparison of pH_o Dependence of the Extracellular Sulfate Dissociation Constant, K_o^S, with that of the Extracellular Iodide Dissociation Constant, K_o^I.

pH_o	K_o^I	$K_o^I/K_o^I{}_{pH8.5}$	$(K_o^I/K_o^I{}_{pH8.5})^2$	K_o^S	$K_o^S/K_o^S{}_{pH8.5}$
8.5	0.98	0.98	0.96	1.47	1.05
	1.24	1.24	1.53	1.32	0.95
	0.71	0.71	0.50		
	1.08	1.08	1.16		
Average*	1.003	1.0	1.04	1.40	1.0
9.2	2.90	2.89	8.37	3.31	2.37
	2.30	2.29	5.26	3.30	2.37
Average	2.60	2.59	6.82	3.31	2.37
10	8.13	8.11	65.7	11.3	8.1
	5.66	5.65	31.9	17.9	12.8
	7.31	7.29	53.2	13.1	9.4
	4.82	4.81	23.1		
Average	6.48	6.46	41.8	14.1	10.1‡

K_o^I is the dissociation constant of iodide for the E_o conformation of band 3, taken from Table I of Liu et al. (1996).

*The average value of the parameters in the column at each pH_o.

‡Significantly different from $(K_o^I/K_o^I{}_{pH8.5})^2$, determined by an unpaired *t* test ($P < 0.05$), but not significantly different from $K_o^I/K_o^I{}_{pH8.5}$ ($P = 0.11$).

in the previous paper, however, precise calculations of the expected results for variations of such fixed charge models are impossible at present, and the model in general involves complex interactions of Cl^- and $SO_4^=$ ions in the local region which would probably lead to nonlinearities in the Dixon plots. Because this model is more complex and less predictive than the SBS model, and because it does not seem to fit the data as well, it seems that the alternative SBS model provides a better explanation of the pH_o effects.

pH Dependence of DNDS Inhibition

DNDS, a stilbene derivative with two negative charges, inhibits anion transport by reversibly binding to band 3. At neutral pH_o DNDS seems to act primarily as a competitive (transport site) inhibitor (Fröhlich, 1982). If DNDS binds at or near the substrate binding site, one would expect that the titration of charged residues in or around the substrate binding site would have effects on the dissociation constant for DNDS binding to the E_o conformation, K_e^{DNDS}. Therefore, we tested the effects of external pH on K_e^{DNDS} with constant 150 mM $[Cl_i]$ and pH_i 7.2.

To determine ID_{50} (the concentration which half-inhibits Cl^- exchange) and K_e^{DNDS}, ^{36}Cl effluxes were measured in media of different $[Cl_o]$ (with sucrose replacing Cl^-) with various $[DNDS_o]$. The results were plotted on Dixon plots (1/flux vs [DNDS]) such as Fig. 2, which shows data for pH_o 10.9. The ID_{50} is equal to the negative of the x intercept of the Dixon plot. K_e^{DNDS} is given by the negative of the x coordinate of the intersection point of the Dixon plot lines with different $[Cl_o]$.

The values of ID_{50} and K_e^{DNDS} at various pH_o are shown in Table II. At pH_o 7.2 to 8.5 the K_e^{DNDS} values range from 0.038 to 0.097 μM, very similar to the value of 0.084 ± 0.004 μM reported by Fröhlich (1982), using an optical absorbance technique to measure DNDS binding. Because Fröhlich's data were obtained by using citrate to replace Cl^- and to maintain constant ionic strength, whereas the experiments in Table II had varying ionic strength and no citrate, it seems likely, as discussed in the preceding paper (Liu et al., 1996) in connection with K_o^I, that the effects of ionic strength on K_e^{DNDS} are small, or else that effects of ionic strength on the dissociation constant and on the pK values for the positive sites tend to cancel out in this pH_o range. K_e^{DNDS} increases with pH_o, indicating that the inhibitory potency decreases at higher pH_o. This is consistent with the dramatic reduction in the inhibition of Cl^- exchange by DNDS at pH_o values >10 observed by Wieth and Bjerrum (1983).

If DNDS binds to the transport site, the increase in K_e^{DNDS} with increasing pH_o could be partially or completely the result of the same titration which causes the increase in K_o^I. Fig. 3 shows a comparison of the values of K_e^{DNDS} and K_o^I, divided by their respective values at pH 7.2. From Fig. 3 *A*, it is clear that increasing pH_o from 8 to 10.5 has a much larger effect on K_e^{DNDS} (*open triangles*) than on K_o^I (*solid triangles*). Bjerrum (1992) has also reported unpublished data showing that DNDS affinity is affected at lower pH_o values than is Cl^- affinity. At higher pH_o values, K_e^{DNDS} increases to such an extent that it is difficult to present on a linear scale, and is better seen on a logarithmic plot such as Fig. 3 *B*. By pH_o 11.2, there is a ~700-fold increase in K_e^{DNDS}, compared to only a ~40-fold increase in K_o^I.

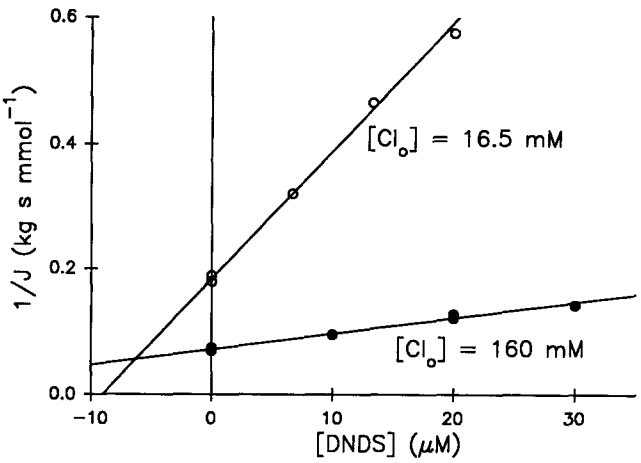

FIGURE 2. Dixon plot of inhibition of Cl^- exchange by external DNDS at pH 10.9. Cl^- exchange fluxes were measured in media with various [DNDS] as described in Methods. (*Open circles*) $[Cl_o]$ = 16.5 mM; (*closed circles*) $[Cl_o]$ = 160 mM. Lines are drawn from best-fit parameters determined by nonlinear least-squares fits as described in Fig. 1. The x coordinate of the intersection point of the lines with different $[Cl_o]$ gives K_e of 6.26 μM.

Competitive and Noncompetitive Effects of DNDS

According to the ping-pong mechanism, the distribution of band 3 among its various forms is a function of $[Cl_i]$ and $[Cl_o]$. In general, the reciprocal of the ID_{50} for an inhibitor such as DNDS is the average of the reciprocals of the dissociation constants of DNDS for each form of band 3 (see Fig. 4 *A*), weighted according to the fraction of band 3 in each form in the absence of inhibitor (Knauf et al., 1992):

$$I/ID_{50} = (E_o/K_e + E_i/K_g + ECl_o/K_f + ECl_i/K_h)/E_t, \quad (5)$$

where E_t is the total concentration of band 3 and K_f, K_g, and K_h are dissociation constants of inhibitor for the ECl_o, E_i, and ECl_i conformations respectively (Fig. 4 *A*). Thus, the ID_{50} will vary with $[Cl_o]$, as the distribution of band 3 among the various conformations changes. If DNDS is an external competitive inhibitor, it can bind only to the E_o conformation of band 3. That is, K_f, K_g,

TABLE II

pH_o Dependence of ID_{50} for DNDS at Various $[Cl_o]$ and Dissociation Constant of DNDS for E_o Conformation, Ke^{DNDS}

pH_o	$K_{1/2o}$ (SE)	$[Cl_o]$	ID_{50} (SE)	K_e^{DNDS}	Experiment
0°C	*mM*	*mM*	*μM*	*μM*	*No.*
7.2	0.31 (0.05)	1	0.18 (0.02)	0.038	66
		148.5	4.29 (0.19)		
		0.5	0.17 (0.04)	0.059	66a
		148.5	4.48 (0.27)		
8.5	1.03 (0.15)	1.1	0.21 (0.05)	0.044	66
		163.4	5.18 (0.40)		
		0.55	0.19 (0.03)	0.097	79
		148.5	7.35 (2.53)		
9.2	2.64 (0.33)	1.1	0.41 (0.09)	0.23	79
		110	5.12 (0.29)		
		0.88	0.62 (0.21)	0.38	80
		110	4.18 (0.20)		
9.9	8.57 (0.97)	11	1.65 (0.18)	0.69	66b
		163.4	7.75 (0.92)		
		11	2.84 (0.07)	1.54	JE4
		163.4	8.59 (0.11)		
10.4	12.1 (2.1)	5.5	2.45 (0.19)	1.69	78
		161.7	14.2 (2.2)		
10.6	25.1 (2.5)	16.5	8.39 (1.51)	5.38‡	JE1
		160.1	23.4 (3.5)		
		16.5	7.47 (0.59)	4.71‡	JE2
		160.1	26.9 (1.7)		
10.9	39.0 (6.5)	16.5	25.5 (2.0)	25.5	66b
		160.1	25.7 (2.0)		
		163.4	25.2 (4.6)	*	66
		160.1	25.0 (5.0)	*	66a
		16.5	11.3 (1.4)	8.38	JE1
		160.1	47.3 (15.3)		
		16.5	16.1 (2.5)	12.0	JE2
		160.1	57.1 (8.3)		
		16.5	9.02 (0.56)	6.26	JE3
		160.1	29.1 (2.3)		
11.2	144.2 (30.4)	16.5	31.8 (6.9)	29.5‡	JE3
		160.1	48.2 (7.9)		
		16.5	35.0 (2.7)	32.4‡	JE4
		160.1	52.1 (4.6)		

* At pH_o 10.9, the ID_{50} values for low $[Cl_o]$ in experiment 66 and 66a are not given because the highest DNDS concentration (0.3 μM) did not significantly inhibit anion transport.

‡ Significantly different ($P < 0.005$) from the grouped data at pH_o 7.2 and 8.5 according to an unpaired t test.

and K_h are infinite or very large, so Eq. 5 reduces to $ID_{50} = K_e(E_t/E_o)$. Thus, the ID_{50} will be much lower with low $[Cl_o]$ than with high $[Cl_o]$, due to the increase in E_o under these conditions (Fröhlich et al., 1983; Fröhlich and Gunn, 1986). For example, when $[Cl_o] = K_{1/2o}$ (the concentration of external Cl^- that gives half-maximal flux), $E_o = E_t/2$.

The results in Table II show strong effects of $[Cl_o]$ on the DNDS ID_{50} at pH_o 7.2, as expected. In the low Cl^- (0.5–1 mM) media, the ID_{50} for DNDS is ~25 times

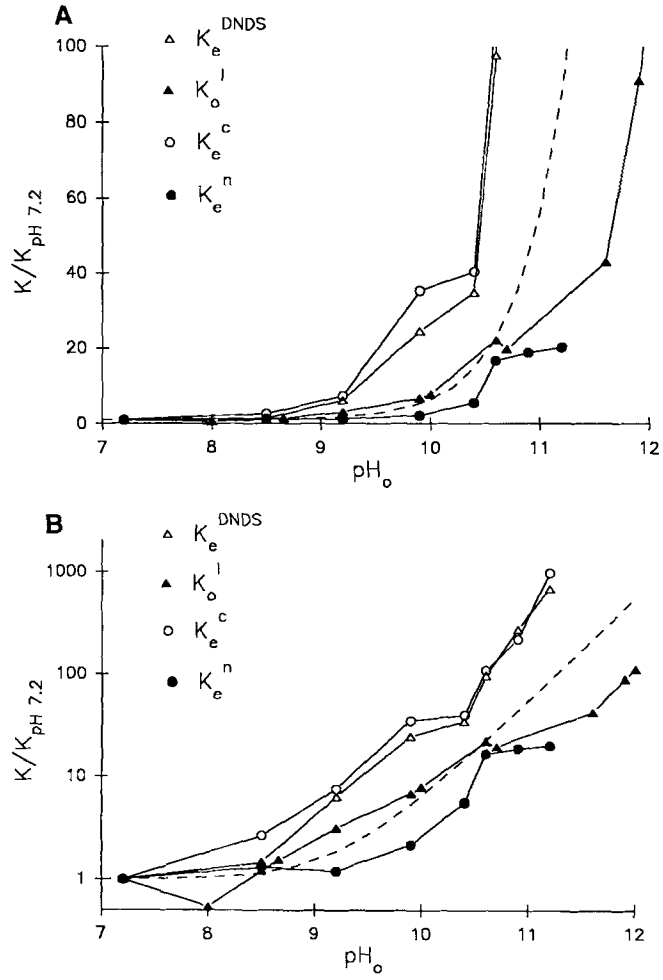

FIGURE 3. Effect of pH_o on K_e^{DNDS}, K_e^c, K_e^n, and K_o^I. (*A*) Linear ordinate; (*B*) logarithmic ordinate. The various constants are expressed as ratios relative to their values at pH_o 7.2. Data for K_e^{DNDS} are from Table II, for K_e^c and K_e^n are from Table III, and for K_o^I are from Liu et al. (1996). The dashed line represents predictions based on a model in which a doubly charged anion is located at the same distance from the titratable sites as I^-, calculated using the two titratable site model in which the completely deprotonated form has negligible affinity for anions, with the pK values given in the preceding paper (Liu et al., 1996).

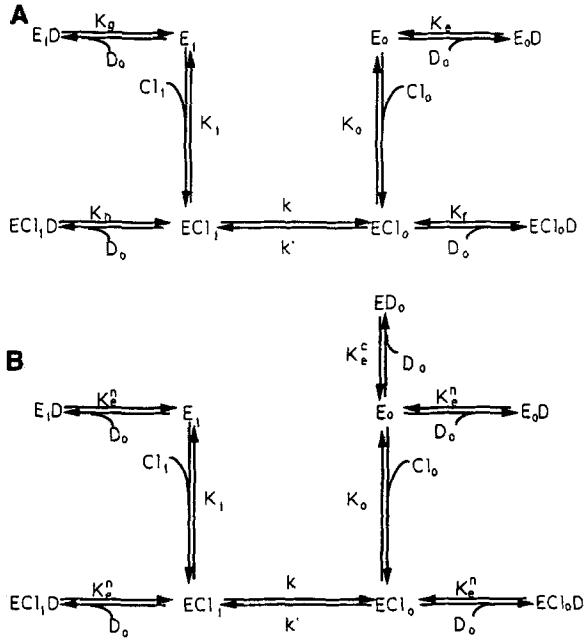

FIGURE 4. (*A*) Model for inhibition of Cl^- exchange by an inhibitor (*D*), which can bind to all of the various forms of band 3. (*B*) Inhibition of Cl^- exchange, assuming that DNDS (*D*) binds to the transport site with dissociation constant K_e^c, and to a noncompetitive site with dissociation constant K_e^n, which is the same regardless of the conformation of band 3.

lower than the ID_{50} in 149 mM Cl^- medium, suggesting that DNDS binds preferentially to the E_o conformation, which is consistent with the idea that DNDS is a competitive inhibitor (Fröhlich, 1982). At higher pH_o, the ID_{50} for DNDS does not increase as much with increasing $[Cl_o]$. In part this is due to the increase in $K_{1/2o}$, which makes Cl^- a less effective competitor, but it also suggests that DNDS can bind to other conformations of band 3 as well as to E_o.

The possibility that DNDS displays some noncompetitive inhibition at high pH_o (and even at lower pH_o values) was tested as follows: if one assumes (Fig. 4 *B*) that DNDS, besides binding to E_o as a competitive inhibitor with dissociation constant K_e^c, can also bind noncompetitively to all forms of band 3 with the same dissociation constant K_e^n, and that the competitive and noncompetitive binding of DNDS to E_o are mutually exclusive, a linear Dixon plot will be obtained as in Fig. 2 and $1/ID_{50}$ will be given by (see Appendix):

$$1/ID_{50} = 1/K_e^n + 1/(K_e^c[1 + [Cl_o]/K_{1/2o}]), \quad (6)$$

where $K_{1/2o}$ is the external half saturation concentration for Cl^- with $[Cl_i]$ kept constant at each pH_o, determined by fitting the Michaelis-Menten equation to the data for flux as a function of $[Cl_o]$. The values of K_e^c and K_e^n, determined by nonlinear fitting of ID_{50} vs $[Cl_o]$, as well as the experimentally measured K_e^{DNDS}, are presented in Table III. K_e^c is approximately equal to K_e^{DNDS}, but is much lower than K_e^n (~120 times lower at pH_o 7.2 and 16 times lower at pH_o 10.4), as expected if the competitive component dominates the overall inhibition.

The competitive component has a different pH dependence from the noncompetitive one, as shown in Table III and in Fig. 3, where K_e^c and K_e^n, divided by their values at pH 7.2, are plotted for comparison with similarly normalized values of K_e^{DNDS} and K_o^I. Like K_e^{DNDS}, K_e^c begins to increase between pH_o 8 and 10 (Fig. 3 *A*), and by pH_o 11.2 reaches a value ~1,000 times larger than its value at pH_o 7.2 (Fig. 3 *B*). In contrast, K_e^n does not increase until pH_o is raised to 9.9, as

TABLE III

Values of K_e^{DNDS}, K_e^c, and K_e^n (Micromolar) as a function of pH_o

pH_o	K_e^{DNDS}	K_e^c	K_e^n
7.2	0.0485	0.0453	5.44
8.5	0.0705	0.120	7.20
9.2	0.305	0.339	6.51
9.9	1.20	1.60	11.7
10.4	1.69	1.83	30.3
10.6	4.74	4.99	90.9
10.9	13.6	10.1	103.
11.2	33.8	45.1	110.

Standard errors for K_e^c and K_e^n were < 30% of the mean, except for one K_e^n value at pH 10.9. Average K_e^{DNDS} values for each pH_o were calculated from Table II; standard errors for $pH_o > 9$ were < 38% of the mean.

shown in Fig. 3 *B*, and the maximum change by pH_o 11.2 is only ~20-fold (Fig. 3 *A*). The different titration profiles for K_e^c and K_e^n fit well with the concept that DNDS binds at different sites in the band 3 molecule for competitive and noncompetitive inhibition.

Because K_e^n (~5 μM at pH_o 7.2) is much higher than K_e^c (Table III), at low concentrations DNDS acts primarily as a competitive inhibitor and the noncompetitive component does not play an important role. However, when DNDS is used at relatively high concentrations, for example, to protect the substrate binding site from chemical modification, the experiments must be interpreted cautiously, because under these conditions DNDS binds to at least one other site (the noncompetitive binding site) besides the transport site. Two recent brief reports provide further evidence that there is a noncompetitive component of DNDS inhibition (Knauf et al., 1993; Aranibar et al., 1994).

pH Dependence of Competitive and Noncompetitive DNDS Binding

If the dissociation constant for DNDS binding to the E_o form of band 3, K_e^{DNDS}, is fitted to a single titratable site model, the pK value is 8.3 ± 0.5. The large standard error probably results from the sharp increase in K_e^{DNDS} with pH_o, the scatter in the high pH_o data, and the failure to observe a plateau at high pH_o. (In fact, the calculated value for the DNDS dissociation constant of the deprotonated form approaches infinity.) A fit to a two-site model, with pK_D fixed at 11.35 (Bjerrum, 1992) gives an apparent pK_C of 8.7 ± 0.3. For K_e^c the one-site model gives a pK_C of 8.3 ± 0.6 and the two-site model gives 9.0 ± 0.2. All of these values fall near the range (8.7–9.5) obtained from Bjerrum's (1992) model and from fits to K_o^I data in the preceding paper (Liu et al., 1996). Thus, the data are consistent with the concept that the same titratable site(s) affect DNDS and I^- binding.

As another test of the hypothesis that DNDS and I^- are affected by the same titratable sites, we calculated the expected pH_o dependence of the dissociation constant for a doubly charged anion that is bound at precisely the same location as I^-. This was done by taking the best-fit parameters for the pH_o dependence of I^- binding, based on a model in which titration of the high-pK site (D) abolishes anion binding affinity (Bjerrum, 1992; Liu et al., 1996), and squaring the value of the dissociation constant with the C residue deprotonated (corresponding to K_+^I), as predicted by Eq. 4. The prediction, shown by the dashed lines in Fig. 3, *A* and *B*, falls well below the observed K_e^{DNDS} and K_e^c values over the entire pH_o range, suggesting that additional titratable positive charges besides those that affect I^- binding influence the competitive binding of DNDS. Evidence that DNDS binds in a region with several positive charges (Passow, 1986) makes this possibility more likely. Moreover, site-directed mutations of Lys-558 and Lys 869 of mouse band 3 (corresponding to Lys-539 and Lys-851 of human band 3) have much larger effects on DNDS affinity than on Cl^- affinity (Wood et al., 1992), consistent with the idea that additional charge interactions are involved in DNDS binding.

The lower-affinity noncompetitive component of DNDS inhibition, K_e^n, fits better to a one or two-titratable site model, with pK's of 9.4 ± 0.5 in either case, although the affinities for the protonated and deprotonated forms are very poorly defined. This is not significantly different from the pK value obtained from the K_o^I data (Liu et al., 1996) or from Bjerrum's model, so the data do not disprove the hypothesis that the same (probably Lys) site may affect both binding of transported substrates and the noncompetitive binding of DNDS. This might seem an unlikely situation, but it is easier to envision if the amino group is actually located several Å from the transport site (see below). On the other hand, a separate group with a similar pK may be responsible for the pH dependence of K_e^n.

pH_o Dependence of External Cl^- Half Saturation $K_{1/2o}$ and Maximum Flux, J^{mo}

The data in Table II for the effect of pH_o on $K_{1/2o}$ are plotted in Fig. 5 (*solid circles*). It is apparent that $K_{1/2o}$ increases dramatically at pH values > 9.[1] According to the ping-pong model for anion exchange (see Appendix and Fröhlich and Gunn, 1986), $K_{1/2o}$ is given by:

[1] The values of $K_{1/2o}$ at pH 7–8.5 are somewhat lower than those previously reported by Gunn and Fröhlich (1979) at pH 7.8. This may be due to the fact that citrate was not used in these experiments to maintain ionic strength. Thus, as discussed in the preceding paper (Liu et al., 1996), competitive effects of citrate were avoided, but the constants are "apparent" in the sense that they apply strictly only to conditions where the ionic strength is allowed to vary with $[Cl_o]$.

$$K_{1/2o} = K_o(k/k')/\{1 + (K_i/[Cl_i]) + (k/k')\}, \quad (7)$$

where K_o and K_i are the dissociation constants for binding of Cl^- to the outward-facing or inward-facing transport sites, respectively, and where k is the rate constant for conversion from the inward-facing ECl_i form to the outward-facing ECl_o form, while k' is the rate-constant for the reverse conformational change (see Fig. 4). Because $[Cl_i]$ is high and constant, the term $K_i/[Cl_i]$ is unlikely to strongly influence $K_{1/2o}$. An increase in $K_{1/2o}$ could, however, reflect an increase in K_o with pH_o, or could be related to either an increase in k or a decrease in k', any one of which would increase the numerator in Eq. 7.

The maximum Cl^- exchange flux, with constant $[Cl_i]$ and with saturating $[Cl_o]$, is given by:

$$J^{mo} = kE_t/\{1 + (K_i/[Cl_i]) + (k/k')\}. \quad (8)$$

J^{mo} is plotted as a function of pH_o in Fig. 5 (*open circles*). Like $K_{1/2o}$, J^{mo} also increases with increasing pH_o, but in this case the increase is smaller and occurs only at pH_o around 11. If Eq. 7 is divided by Eq. 8, one is left with:

$$K_{1/2o}/J^{mo} = K_o/(k'E_t), \quad (9)$$

because the identical denominators of Eq. 7 and 8 cancel out. (This is the reason why, in a ping-pong model [Gunn and Fröhlich, 1979], the ratio $K_{1/2o}/J^{mo}$ is independent of $[Cl_i]$.) When the ratio $K_{1/2o}/J^{mo}$ is plotted against pH_o (Fig. 6, *solid circles*), there is a large increase with increasing pH_o. This increase must be related either to an increase in K_o or to a decrease in k' or both, because E_t, the total amount of band 3, remains constant.

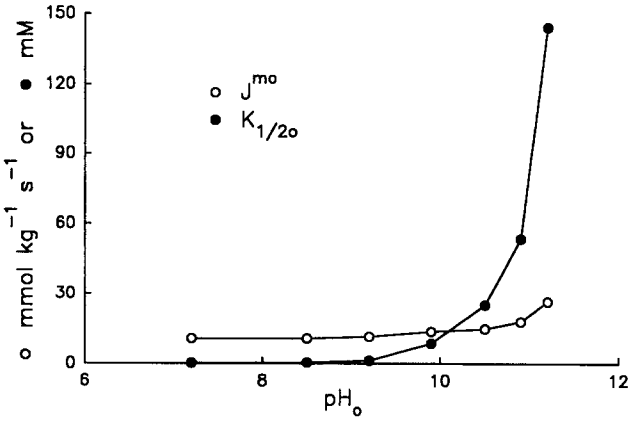

FIGURE 5. Effect of pH_o on the half-saturation constant ($K_{1/2o}$) and on the maximum flux (J^{mo}), determined by varying $[Cl_o]$ with constant $[Cl_i]$. Cells were preequilibrated with ^{36}Cl at pH 7.2, so $[Cl_i]$ was ~150 mM. $K_{1/2o}$ (*solid circles*) and J^{mo} (*open circles*) were determined from best fits of the Michaelis-Menten equation to the flux vs $[Cl_o]$ data by using Enzfitter or Kaleidagraph (Synergy Software).

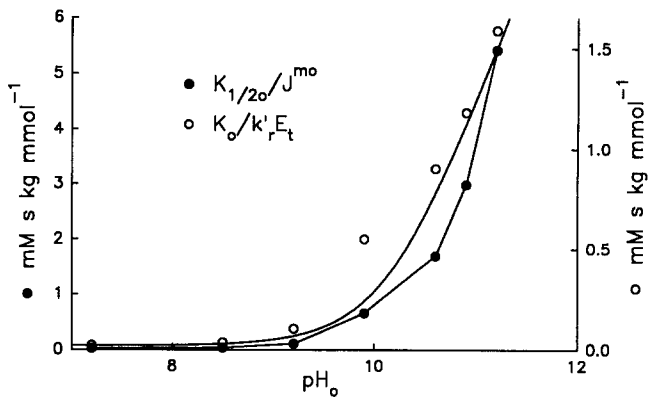

FIGURE 6. Effect of pH_o on $K_{1/2o}/J^{mo}$ (*solid circles*) and on $K_o/(k'_rE_t)$ (*open circles*). $K_{1/2o}$ and J^{mo} are from Fig. 5. According to Eq. 6, $K_{1/2o}/J^{mo}$ should equal $K_o/(k'E_t)$. To obtain an estimate of the effects of pH_o on K_o which is corrected for possible variations of k' with pH_o, we multiplied $K_{1/2o}/J^{mo}$ at each pH_o by the calculated ratio of k' to k' at pH 8.5 (k'_r), determined as described in Fig. 7 of Liu et al. (1996). This gives $K_o/(k'_rE_t)$ which, since k'_r and E_t are constants, should reflect the effects of pH_o on K_o. The solid line through the open circles is a least-squares best-fit (using Origin) to a two titratable site model, with each point weighted as its inverse, including both our data and Bjerrum's (1992) data, as shown in Fig. 7.

In the preceding paper (Liu et al., 1996), we calculated the pH_o dependence of k', relative to its value at pH 8.5, k'_r, based on the assumption that external pH has the same effects on Cl^- binding as on I^- binding. If we multiply equation 6 by k'/k'_r, we obtain:

$$(K_{1/2o}/J^{mo})(k'/k'_r) = K_o/(k'_rE_t) \quad (10)$$

Because all of the terms on the right-hand side are constants except K_o, a plot of this function (Fig. 6, *open circles*) should indicate the effects of pH_o on K_o.

These observations complement and are consistent with Bjerrum's (1992) report that J^{mo} increases slightly as pH_o is raised >11, that $K_{1/2o}$ increases dramatically with pH_o, and that $K_{1/2o}/J^{mo}$ tends to increase 10-fold for a 1-U change in pH at high pH_o. In fact, when Bjerrum's data for $K_{1/2o}/J^{mo}$ are multiplied by the k'/k'_r data from the preceding paper (Liu et al., 1996), the resulting K_o/k'_rE_t values (Fig. 7, *solid circles*) fit well with those in Fig. 6 (*open circles* in Fig. 7).

When all of the K_o/k'_rE_t data are fitted to a two titratable site model (assuming no Cl^- binding to the completely deprotonated form), keeping the dissociation constant for the neutral form at the measured value of 0.02, we obtain $pK_C = 8.8 \pm 0.6$ and $pK_D = 12.1 \pm 0.5$, in reasonable agreement with the pK values (9.3 ± 0.3 and 12.7 ± 0.3) determined by fitting the K_o^1 data to the same model (Liu et al., 1996). The K_o/k'_rE_t value for the alkaline form, with one residue deprotonated, is very poorly determined but is ~1.8 ± 1.3. The mean value

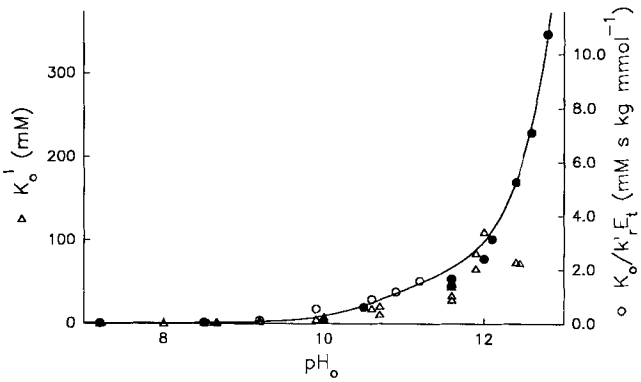

FIGURE 7. Comparison of effects of pH_o on $K_o/(k'_rE_t)$ and K_o^I. The left axis shows K_o^I values (*open triangles*) taken from Fig. 3 and Table I of the preceding paper (Liu et al., 1996). The right axis shows values of $K_o/(k'_rE_t)$ from Fig. 6 (*open circles*) and calculated from Fig. 13 of Bjerrum (1992) (*solid circles*), using the conversion factor 0.38 pmol/cm^{-2} s^{-1} = 1 mmol kg^{-1} min^{-1} (Gunn and Fröhlich, 1989). The solid line represents a best fit to a two titratable site model assuming negligible binding to the completely deprotonated form. The $K_o/(k'_rE_t)$ value for the protonated form is fixed at 0.02 mM s kg mmol^{-1}, the value for the alkaline form with the C residue deprotonated is 1.8 ± 1.3 mM s kg mmol^{-1}, the pK_C value is 8.8 ± 0.6, and the pK_D value is 12.1 ± 0.5. The axes for $K_o/(k'_rE_t)$ and K_o^I are scaled so that the values match at pH_o 7.2.

corresponds to a 90-fold increase in K_o, not significantly different from the 70-fold increase seen for K_o^I.

Fig. 7 also shows a direct comparison of the $K_o/(k'_rE_t)$ data with the K_o^I data. When the scales are adjusted for the different magnitude of each parameter at pH_o 7.2, it appears that the major difference is that some of the K_o^I values, particularly at pH_o 11.6 and 12.4, fall somewhat below the $K_o/(k'_rE_t)$ values. Because K_o should be the only pH-dependent variable in $K_o/(k'_rE_t)$, this seems to violate the assumption that pH_o has parallel effects on Cl^- and I^- dissociation constants. Most of the apparent discrepancy, however, seems to be related to scatter in the K_o^I values; for example, the fit of the K_o^I data to the Cl^- data is much better around pH_o 12 than at pH_o 12.4. Also, as mentioned above, fits to the data indicate no significant difference in the effect of deprotonation of the low-pK C residue on $K_o/(k'_rE_t)$ as compared to K_o^I, so the assumption that I^- and Cl^- affinities are affected similarly by pH_o is at least approximately valid.

Even if the data in Fig. 7 are taken at face value, the additional increase in $K_o/(k'_rE_t)$ relative to that for K_o^I would be only about twofold. If we make the corresponding assumption that the alkaline form of band 3 (with the C group deprotonated) exhibits twice as large an increase in K_o (for Cl^-) as in K_o^I, Eq. T2.6 in the preceding paper (Liu et al., 1996) must be replaced by:

$$T_b = K_{o,+}/K_+^I = 2T = 2K_{o,++}/K_{++}^I \qquad (11)$$

where T_b represents the ratio of Cl^- to I^- affinities for the alkaline state and the other terms have the meanings defined in the preceding paper. Insertion of this equation yields the final result that the term (k'_+/k'_{++}) in Eq. 4 of the preceding paper is replaced by $(k'_+/k'_{++})/2$. Thus, the fit to the Dixon plot slope data gives half of (k'_+/k'_{++}), rather than (k'_+/k'_{++}). In general, the value obtained from the fit is equal to T/T_b (k'_+/k'_{++}). Thus, the true value of (k'_+/k'_{++}) would be 0.28 instead of 0.14. Such a change would not substantially affect the conclusions drawn in the preceding paper.

Effects of BSSS on $K_{1/2o}$ and J^{mo}

To see whether or not particular externally-accessible lysines are involved in external anion binding, we used BSSS, a nonpenetrating cross linking reagent (Staros and Kakkad, 1983) which probably reacts with the same Lys residues with which H_2DIDS reacts (Jennings et al., 1985; Okubo et al., 1994). BSSS has the advantage that it does not introduce new charged groups into band 3, as do the disulfonic stilbenes, and that upon reaction with an amino group, the pK is changed so that the positive charge is absent at neutral pH. Also, since BSSS does not completely inhibit anion exchange, the modified transport system may be studied. In fact, although BSSS inhibits Cl_i-Br_o exchange by at least 90% at pH_o > 8, Cl_i-Br_o exchange of BSSS treated cells could be activated by lowering external pH (Jennings et al., 1985). In BSSS treated cells the half-saturation constant for extracellular Br^- was higher than the corresponding $K_{1/2}$ for control cells, indicating that reaction with BSSS decreases substrate affinity (Jennings et al., 1985).

Cl^- exchange was inhibited by ~90% at pH_o 7.2 in BSSS treated cells (Knauf and Spinelli, 1995), but the remaining flux could still be measured easily. Therefore, we examined how BSSS treatment affects the pH dependence of substrate binding to band 3. Because Cl_i-I_o exchange is stimulated by BSSS (Jennings et al., 1985), we were unable to measure K_o^I in BSSS treated cells, since the Dixon plot intersection technique requires that Cl_i/Cl_o exchange be much faster than Cl_i/I_o exchange (Knauf and Brahm, 1989; Liu et al., 1996). We chose instead to measure the effects of pH_o on the apparent half-saturation constant for external Cl^-, $K_{1/2o}$, and on the apparent maximum flux, J^{mo}, in BSSS-treated cells with a constant pH_i (7.2) and constant $[Cl_i]$ (~150 mM), as described above for control cells.

J^{mo} (*solid circles* in Fig. 8) is much lower in BSSS-treated cells than in control cells (compare *solid circles* in Fig. 8 with *open circles* in Fig. 5; note difference in scale), and remains fairly constant above pH_o 8.7, decreasing slightly above pH 11. This suggests (Eq. 8) that k is greatly reduced in BSSS-treated cells. The increase in J^{mo} at low pH_o (6.4) is similar to the behavior that is seen for Cl_i/Br_o exchange, where more acidic pH_o acti-

vates transport with a pK of ~7 (Jennings et al., 1985). Fig. 8 also shows data for $K_{1/2o}$ and $K_{1/2o}/J^{mo}$ for BSSS-treated cells as a function of pH_o. Even at the lowest pH values shown, $K_{1/2o}$ (*open squares*) is much higher than in control cells (Fig. 5). This probably reflects an increase in K_o (Eq. 7), which could be explained either if neutralization of an amino group reduces the favorable electrostatic free energy for Cl^- binding or if BSSS sterically or allosterically hinders Cl^- binding. If k/k' is assumed to remain constant, the increase in $K_{1/2o}$ would correspond to a 32-fold increase in K_o relative to untreated cells around pH_o 8.5–8.7.

When $K_{1/2o}/J^{mo}$ is plotted (*open circles* in Fig. 8), it is clear that the value is much greater than for the control (*solid circles* in Fig. 6; note difference in scale) at all pH values. At pH 8.7, for example, with BSSS $K_{1/2o}/J^{mo}$ is ~2,400 times larger than for the control. This could be explained by the combined effects of a 32-fold increase in K_o, as discussed above, and a 75-fold decrease in k' (Eq. 9).

The increase in both $K_{1/2o}$ and $K_{1/2o}/J^{mo}$ as pH_o is increased from 8.7 to 10 could be due to either a further increase in K_o or a decrease in k' (Eq. 7 and 9). In either case, the data indicate that a low-pK titration is preserved in BSSS-treated cells, suggesting that the C residue does not react with BSSS. If we fit the $K_{1/2o}/J^{mo}$ data to a two titratable site model, with pK_C fixed at 8.8 and pK_D at 11.35 (Bjerrum's (1992) parameters for relatively low ionic strength media), the fit is not too good for the left limb of the bell-shaped curve (*dashed line* in Fig. 9). An even poorer fit (not shown) is obtained if the value of 9.3 from the preceding paper (Liu et al., 1996) is used for pK_C. If pK_C is treated as a variable, the best-fit value is 7.5 ± 0.2, and a rather good fit is obtained (*solid line* in Fig. 9). The different value for pK_C does not rule out the possibility that the C residue remains titratable after BSSS treatment, because BSSS might alter the environment of the residue and hence might lower its apparent pK.

Surprisingly, both $K_{1/2o}$ and $K_{1/2o}/J^{mo}$ in BSSS-treated cells decrease markedly at $pH_o > 10$ (Fig. 8). The simplest explanation for this (Eqs. 7 and 9) is that K_o decreases, but an increase in k' cannot be ruled out. At $pH_o > 11$, $K_{1/2o}$ for BSSS-treated cells is actually lower than for control cells (compare *open squares* in Fig. 8 with *solid circles* in Fig. 5), implying that under these conditions the BSSS-modified band 3 has a higher apparent affinity for Cl^- than does unmodified band 3. As shown in Fig. 9, this behavior is compatible with a two-site model in which the second titration lowers the apparent dissociation constant for Cl^-, rather than raising it as in control cells.

The ability of the cross-linker BSSS to prevent the decrease in apparent Cl^- affinity that normally occurs at high pH might indicate that the increasing negative charge on band 3 causes electrostatic repulsion that "opens up" the band 3 structure and perturbs the external anion binding site. The BSSS intramolecular cross-link would act to stabilize the normal structure and prevent this effect. As the effects of pH_o are completely reversible (Wieth and Bjerrum, 1982), any changes in structure which take place must also be reversible. On the other hand, it is possible that the decrease in $K_{1/2o}$ and in $K_{1/2o}/J^{mo}$ is caused in whole or in part by an increase in k', that would decrease the number of outward-facing sites and thereby decrease the apparent $K_{1/2o}$ (which is equivalent to the $[Cl_o]$ at which half of the band 3 molecules are in

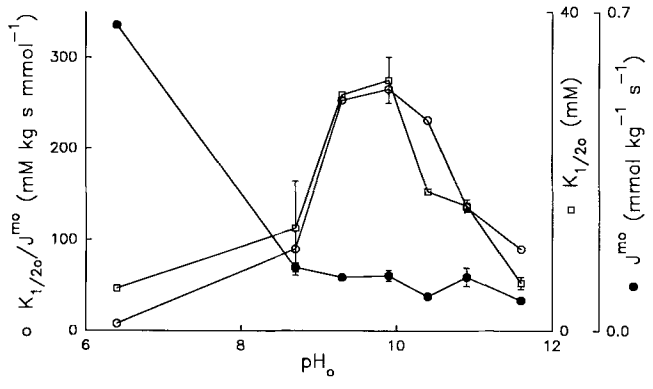

FIGURE 8. Effects of pH_o on $K_{1/2o}$ (*open squares*), J^{mo} (*solid circles*), and $K_{1/2o}/J^{mo}$ (*open circles*) in BSSS-treated cells. Fluxes were calculated from Cl^- exchange rate-constants, using a value of 181.5 mmol Cl^-/kg dry weight. Bars indicate range of two experiments; other points are single experiments. (Error bars for $K_{1/2o}/J^{mo}$ are shown in Fig. 9.) Flux vs $[Cl_o]$ data were used to determine $K_{1/2o}$ and J^{mo} from nonlinear fits to the Michaelis-Menten equation as described in Fig. 5; $[Cl_i]$ was ~150 mM.

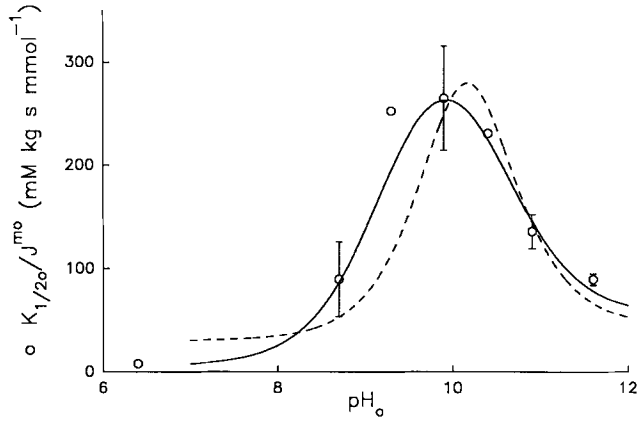

FIGURE 9. Fits of $K_{1/2o}/J^{mo}$ in BSSS-treated cells to a two titratable site model. Dashed line represents best fit to a model with pK_C fixed at 8.8 and pK_D fixed at 11.35 (Bjerrum, 1992), with $K_{1/2o}/J^{mo}$ of 30 ± 2, 980 ± 230, and 44 ± 3 mM kg s mmol^{-1} for the doubly protonated, singly protonated, and unprotonated forms. Solid line depicts best fit with pK_D fixed at 11.35 (Bjerrum, 1992) and with pK_C = 7.45 ± 0.2, and $K_{1/2o}/J^{mo}$ values of 6 ± 3, 370 ± 30, and 54 ± 4 mM kg s mmol^{-1} for the different titration states.

the E_o form; this needs to be lower to increase E_o sufficiently if there is less E_o at high $[Cl_o]$).

Identity of the Charged Residues

Structural models of band 3 (Tanner et al., 1988; Lux et al., 1989; Wood, 1992) indicate that there are many Lys and Arg residues in the transmembrane segments or in the loops adjacent to them which could function as the charges that bind external anions. At least one of these, Lys-430, seems unlikely because it is the site of reaction of eosin-5-maleimide, which is a noncompetitive inhibitor and which therefore must not bind to the external transport site (Knauf et al., 1993; Liu and Knauf, 1993; Liu et al., 1995). However, as discussed in the preceding paper (Liu et al., 1996) the amino group that increases substrate affinity could be > 4.4 Å from the anion binding site (assuming a dielectric constant of 30 in the region near the transport site), so it might be possible for an inhibitor to react with the amino group and still not block the transport site. Lys-851, which reacts with a transported substrate, pyridoxal phosphate (Kawano et al., 1988) and with a competitive inhibitor, H_2DIDS (Okubo et al., 1994), would seem to be a good candidate. The fact that transport can proceed even if the corresponding Lys in the mouse band 3 is altered by site-directed mutation (Wood et al., 1992) fits with the idea that this charge increases anion affinity, but is not essential for transport. Jennings et al. (1985), however, have interpreted the effects of BSSS on reductive methylation of this Lys as indicating that BSSS reacts with "Lys-b," now known to be Lys-851 (Okubo et al., 1994). The observation of a low-pK titration in BSSS-treated cells would, therefore, suggest that Lys-851 is not the titratable Lys. Passow (1986) has also argued that the H_2DIDS-reactive lysines are not directly involved in substrate binding. There are, however, several other candidate lysines in band 3, as well as several arginines that might be the high-pK residue. Much further work with chemical probes and site-directed mutagenesis will be necessary to identify the functionally-important residues and to determine their precise role in transport.

APPENDIX

Determination of K_e^n and K_e^c for DNDS from ID_{50} and $[Cl]_o$

The assumption here is that DNDS inhibits anion transport by binding competitively to the E_o form of band 3 with a dissociation constant of K_e^c and noncompetitively to E_o, E_i, ECl_o, and ECl_i with the same dissociation constant, K_e^n (Fig. 4 *B*), where $K_e^c = [E_o]\cdot[D_o]/[ED_o]$ and

$$K_e^n = [E_o]\cdot[D_o]/[E_oD] = [ECl_o]\cdot[D_o]/[ECl_oD] = [ECl_i]\cdot[D_o]/[ECl_iD] = [E_i]\cdot[D_o]/[E_iD]. \quad (A1.1)$$

Subscripts *i* and *o* represent the band 3 conformations with the transport site facing the cytoplasmic or extracellular side of the membrane, respectively. DNDS binds to E_o to form ED_o (in competition with substrates) or to form E_oD as a noncompetitive inhibitor (Fig. 4 *B*). The Cl^- dissociation constants for the E_o form, K_o, and for the E_i form, K_i, are:

$$K_o = [E_o]\cdot[Cl_o]/[ECl_o], \quad K_i = [E_i]\cdot[Cl_i]/[ECl_i]. \quad (A1.2)$$

The Cl^- efflux and influx are:

$$J_o = k\cdot[ECl_i], J_i = k'\cdot[ECl_o], \text{ and } J_o = J_i. \quad (A1.3)$$

The maximum flux, J_m, is the flux when all of the band 3 molecules are either in the ECl_i or ECl_o form, that is, $E_t = ECl_o + ECl_i$, so:

$$J_m = k\cdot E_t/(1 + k/k'). \quad (A1.4)$$

The total amount of band 3 molecules, E_t, is:

$$[E_t] = [E_i] + [E_o] + [ECl_o] + [ECl_i] + [E_iD] + [E_oD] + [ED_o] + [ECl_oD] + [ECl_iD] \quad (A1.5)$$

Substituting Eqs. A1.1–A1.3 into A1.5:

$$E_t = [ECl_i]\cdot F,$$

where

$$F = ((1 + K_o/[Cl_o])\cdot k/k' + 1 + K_i/[Cl_i])\cdot(1 + [D_o]/K_e^n) + k\cdot[D_o]\cdot K_o/(k'\cdot K_e^c[Cl_o]). \quad (A1.6)$$

Therefore, the flux $J = k\cdot[ECl_i] = k\cdot E_t/F = J_m\cdot(1 + k/k')/F$
and

$$1/J = F/(J_m\cdot[1 + k/k']). \quad (A1.7)$$

From Eq. A1.7, the ID_{50} for DNDS is:

$$ID_{50} = \{(1 + K_o/[Cl_o])\cdot k/k' + K_i/[Cl_i] + 1\}/(1 + K_o/[Cl_o])\cdot k/(k'\cdot K_e^n) + (1 + K_i/[Cl_i])/\{K_e^n + k\cdot K_o/(k'\cdot[Cl_o]\cdot K_e^c)\}. \quad (A1.8)$$

Since the external Cl^- half saturation constant, $K_{1/2o}$, is equal to $(K_o\cdot k/k')/(1 + k/k' + K_i/[Cl_i])$, the reciprocal of Eq. A1.8 becomes:

$$1/ID_{50} = 1/K_e^n + 1/\{K_e^c\cdot(1 + [Cl_o]/K_{1/2o})\}. \quad (A1.9)$$

Factors Which Influence $K_{1/2o}$ and J^{mo}

For a ping-pong model of Cl^- exchange such as that depicted in Fig. 4, with no inhibitors present, if the ion

binding and dissociation steps are rapid compared to the ion translocation steps, the unidirectional efflux is given by (see Fröhlich and Gunn, 1986; Knauf et al., 1989):

$$J = kE_t/\{1 + K_i/[Cl_i] + k/k' + (K_o/[Cl_o])(k/k')\} \quad (A2.1)$$

where E_t is the total amount of band 3 and the other parameters are as defined in Fig. 4. If $[Cl_o]$ is maximal, the rightmost term in (A2.1) vanishes. Thus, J^{mo}, the flux with maximal $[Cl_o]$ and constant $[Cl_i]$ becomes:

$$J^{mo} = kE_t/(1 + K_i/[Cl_i] + k/k') \quad (A2.2)$$

which is text Eq. 8. With constant $[Cl_i]$, the $[Cl_o]$ which gives half-maximal flux is obtained by replacing $[Cl_o]$ with $K_{1/2o}$ and then setting the rightmost term in (A2.1) equal to the other three terms in the right-hand parenthesis, because under these conditions the denominator will be twice the value when $[Cl_o]$ is maximal, meaning that the flux will be half of the maximal flux (since the numerator is constant):

$$K_{1/2o} = K_o(k/k')/(1 + K_i/[Cl_i] + k/k') \quad (A2.3)$$

This is text Eq. 7.

The authors gratefully acknowledge Dr. Gordon Harnadek and Ms. Gail Sooknarine for assistance in performing the experiments, Drs. George Kimmich and Ian G. Macara for advice, and Drs. Poul Bjerrum and Otto Fröhlich for providing unpublished results. We also wish to thank one of the reviewers of this paper for helpful suggestions regarding analysis of the data, particularly concerning effects of BSSS.

This work was supported by NIH (NIDDK) grant DK27495.

Original version received 24 January 1994 and accepted version received 30 October 1995.

REFERENCES

Aranibar, N., C. Ostermeier, B. Legrum, H. Rüterjans, and H. Passow. 1994. Influence of stilbene disulfonates on the accessibility of the substrate-binding site for anions in the band 3 protein (AEB1). *Renal Physiol. Biochem.* 17:187–189.

Bjerrum, P. J. 1992. The human erythrocyte anion transport protein, band 3. Characterization of exofacial alkaline titratable groups involved in anion binding/translocation. *J. Gen. Physiol.* 100:301–339.

Fröhlich, O. 1982. The external anion binding site of the human erythrocyte anion transporter: DNDS binding and competition with chloride. *J. Membr. Biol.* 65:111–123.

Fröhlich, O., and R. B. Gunn. 1986. Erythrocyte anion transport: the kinetics of a single-site obligatory exchange system. *Biochim. Biophys. Acta.* 864:169–194.

Fröhlich, O., and R. B. Gunn. 1987. Interactions of inhibitors on anion transporter of human erythrocyte. *Am. J. Physiol. (Cell Physiol.)* 252:C153–C162.

Fröhlich, O., C. Leibson, and R. B. Gunn. 1983. Chloride net efflux from intact erythrocytes under slippage conditions. Evidence for a positive charge on the anion binding/transport site. *J. Gen. Physiol.* 81:127–152.

Gabler, R. 1978. Electrical Interactions in Molecular Biophysics: An Introduction. Academic Press, New York.

Gunn, R. B., and O. Fröhlich. 1979. Asymmetry in the mechanism for anion exchange in human red blood cell membranes. Evidence for reciprocating sites that react with one transported anion at a time. *J. Gen. Physiol.* 74:351–374.

Gunn, R. B., and O. Fröhlich. 1989. Methods and analysis of erythrocyte anion fluxes. *In* Methods in Enzymology, Vol. 173. S. Fleischer and B. Fleischer, editors. Academic Press, Inc., San Diego, California. 54–80.

Jennings, M. L., R. Monaghan, S. M. Douglas, and J. S. Nicknish. 1985. Functions of extracellular lysine residues in the human erythrocyte anion transport protein. *J. Gen. Physiol.* 86:653–669.

Kawano, Y., K. Okubo, F. Tokunaga, T. Miyata, S. Iwanaga, and N. Hamasaki. 1988. Localization of the pyridoxal phosphate binding site at the COOH-terminal region of erythrocyte band 3 protein. *J. Biol. Chem.* 263:8232–8238.

Knauf, P. A., and J. Brahm. 1989. Functional asymmetry of the anion exchange protein, capnophorin: effects on substrate and inhibitor binding. *In* Methods in Enzymology, Vol. 173. S. Fleischer and B. Fleischer, editors. Academic Press, New York. 432–453.

Knauf, P. A., D. Restrepo, S. J. Liu, N. M. Raha, L. J. Spinelli, F.-Y. Law, B. Cronise, R. B. Snyder, and L. Romanow. 1992. Mechanisms of substrate binding, inhibitor binding, and ion translocation in band 3 and band 3-related proteins. *In* Progress in Cell Research, Vol. 2. E. Bamberg and H. Passow, editors. Elsevier, Amsterdam. 35–44.

Knauf, P. A., E. A. Ries, L. A. Romanow, S. Bahar, and E. S. Szekeres. 1993*a*. DNDS (4,4′-dinitro-stilbene-2,2′-disulfonate) does not act as a purely competitive inhibitor of red blood cell band 3-mediated anion exchange. *Biophys. J.* 64:A307.(Abstr.)

Knauf, P. A., S. Ship, L. Breuer, L. McCulloch, and A. Rothstein. 1978. Asymmetry of the red cell anion exchange system. Different mechanisms of reversible inhibition by *N*-(4-azido-2-nitrophenyl)-2-aminoethylsulfonate (NAP-taurine) at the inside and outside of the membrane. *J. Gen. Physiol.* 72:607–630.

Knauf, P. A., and L. J. Spinelli. 1995. NIP- and NAP-taurine bind to external modifier site of AE1 (band 3), at which iodide inhibits anion exchange. *Am. J. Physiol. (Cell Physiol.)* 269:C410–C416.

Knauf, P. A., L. J. Spinelli, and N. A. Mann. 1989. Flufenamic acid senses conformation and asymmetry of human erythrocyte band 3 anion transport protein. *Am. J. Physiol. (Cell Physiol.)* 257:C277–C289.

Knauf, P. A., N. M. Strong, J. Penikas, R. B. Wheeler, Jr., and S. J. Liu. 1993*b*. Eosin-5-maleimide inhibits red cell Cl^- exchange at a noncompetitive site that senses band 3 conformation. *Am. J. Physiol. (Cell Physiol.)* 264:C1144–C1154.

Ku, C. P., M. L. Jennings, and H. Passow. 1979. A comparison of the inhibitory potency of reversibly acting inhibitors of anion transport on chloride and sulfate movements across the human red blood cell membrane. *Biochim. Biophys. Acta.* 553:132–141.

Liu, D., S. D. Kennedy, and P. A. Knauf. 1995. ^{35}Cl Nuclear magnetic resonance line broadening shows that eosin-5-maleimide does not block the external anion access channel of band 3. *Biophys. J.* 69:399–408.

Liu, S. J., and P. A. Knauf. 1993. Lys-430, site of irreversible inhibition of band 3 Cl^- flux by eosin-5-maleimide, is not at the transport site. *Am. J. Physiol. (Cell Physiol.)* 264:C1155–C1164.

Liu, S. J., Y. Law, and P. A. Knauf. 1996. Effects of external pH on substrate binding, and on the inward chloride translocation rate-constant of band 3. *J. Gen. Physiol.* 107:271–291.

Lux, S. E., K. M. John, R. R. Kopito, and H. F. Lodish. 1989. Cloning and characterization of band 3, the human erythrocyte anion-exchange protein (AE1). *Proc. Natl. Acad. Sci. USA.* 86:9089–9093.

Milanick, M. A., and R. B. Gunn. 1982. Proton-sulfate co-transport. Mechanism of H^+ and sulfate addition to the chloride transporter of human red blood cells. *J. Gen. Physiol.* 79:87–113.

Milanick, M. A., and R. B. Gunn. 1986. Proton inhibition of chloride exchange: asynchrony of band 3 proton and anion transport sites? *Am. J. Physiol. (Cell Physiol.)* 250:C955–C969.

Okubo, K., D. Kang, N. Hamasaki, and M. L. Jennings. 1994. Red blood cell band 3: Lysine 539 and lysine 851 react with the same H_2DIDS (4,4′-diisothiocyanodihydrostilbene-2,2′-disulfonic acid) molecule. *J. Biol. Chem.* 269:1918–1926.

Passow, H. 1986. Molecular aspects of band 3 protein-mediated anion transport across the red blood cell membrane. *Rev. Physiol. Biochem. Pharmacol.* 103:61–223.

Schnell, K. F., S. Gerhardt, and A. Schoppe-Fredenburg. 1977. Kinetic characteristics of the sulfate self-exchange in human red blood cells and red blood cell ghosts. *J. Membr. Biol.* 30:319–350.

Shami, Y., A. Rothstein, and P. A. Knauf. 1978. Identification of the Cl^- transport site of human red blood cells by a kinetic analysis of the inhibitory effects of a chemical probe. *Biochim. Biophys. Acta.* 508:357–363.

Staros, J. V., and B. P. Kakkad. 1983. Cross-linking and chymotryptic digestion of the extracytoplasmic domain of the anion exchange channel in intact human erythrocytes. *J. Membr. Biol.* 74:247–254.

Tanner, M. J. A., P. Martin, and S. High. 1988. The complete amino acid sequence of the human erythrocyte membrane anion-transport protein deduced from the cDNA sequence. *Biochem. J.* 256: 703–712.

Wieth, J. O., and P. J. Bjerrum. 1982. Titration of transport and modifier sites in the red cell anion transport system. *J. Gen. Physiol.* 79:253–282.

Wieth, J. O., and P. J. Bjerrum. 1983. Transport and modifier sites in capnophorin, the anion transport protein of the erythrocyte membrane. *In* Structure and Function of Membrane Proteins. E. Quagliariello and F. Palmieri, editors. Elsevier Science Publishers B.V. 95–106.

Wood, P. G. 1992. The anion exchange proteins: homology and secondary structure. *In* Progress in Cell Science, Vol. 2. E. Bamberg and H. Passow, editors. Elsevier Science Publishers, Amsterdam. 325–352.

Wood, P. G., H. Müller, M. Sovak, and H. Passow. 1992. Role of Lys 558 and Lys 869 in substrate and inhibitor binding to the murine band 3 protein: A study of the effects of site-directed mutagenesis of the band 3 protein expressed in the oocytes of *Xenopus laevis*. *J. Membr. Biol.* 127:139–148.